Oda et al. Iraqi Journal of Science, 2023, Vol. 64, No. 8, pp: 3748- 3762
DOI: 10.24996/ijs.2023.64.8.3

ISSN: 0067-2904

Photocatalytic Decolorization of Crystal Violate Dye Solution by ZnO/MWCNT Nanocomposite

Amjed M. Oda[1*], Fadhel Y Khudheyer [2], Ehab K. Obaid [3]
[1] *Science Dept., Basic Education College, University of Babylon, Babylon, Iraq*
[2] *Department of Medical laboratory technology, Al-Zahrawi university college, Karbalaa , Iraq.*
[3] *Soil and Water Resources Sciences, Faculty of Agriculture, Al-Qasim Green University, Babylon, .Iraq*

Received: 31/3/2022 Accepted: 1/11/2022 Published: 30/8/2023

Abstract:

By extracting crystal violate dye (CV) from its aqueous solution, the photocatalytic decolorization performance of ZnO/MWCNT nanocomposite was evaluated. The nanocomposite was prepared by precipitation of ZnO and incorporates on the surface of Multi-Walled Carbon Nanotubes (MWCNT). ZnO nanoparticles were synthesized using the sol gel process with MWCNT acting as a template. They were then analyzed by XRD, SEM, and TEM, which revealed how the shape of the spherical nano ZnO interacts with the point of zero charge (pzc), which allows us to see the physical attributes. In the dipping photoreactor, which included a slurry of dye solution and ZnO/MWCNT nanocomposite, the effectiveness of decolorization was assessed. The photodecolorization was studied for CV dye in aqueous solution at different conditions: The effect of time, weight of catalyst, concentration of dye, temperature, the initial pH of dye solution and addition of $S_2O_8^{2-}$ to show the optimum condition of this process. The main results were the synthesis of incorporated ZnO on MWCNT surface with 10-20 nm with high photodecolorization against CV dye. Full decolorization reached at 90 min and 89.8% decolorization at the half time of reaction. ZnO/MWCNT weight of 0.06 gm per 100 mL was optimum for photodecolorization. The photocatalytic reaction was more efficient in the deceasing of CV concentration and obeys the Langmuir-Hinshelwood kinetic, while the photodecolorization was not less than 95% in pH range 6-10.Also, the photocatalytic reaction was effected in the presence of $S_2O_8^{2}$-, where the photodecolorization was more efficient.

Keywords: Photocatalytic reaction, ZnO, MWCNT, Nanocomposite, Photodecolorization.

الازالة اللونية الضوئية المحفزة لمحلول صبغة الكريستال البنفسجي بواسطة المتراكب النانوي ZnO/MWCNT

امجد عودة* ، فاضل خضير ، ايهاب عبيد
[1]قسم العلوم ، كلية التربية الاساسية ، جامعة بابل ، بابل ، العراق
[2]قسم تقنيات المختبرات الطبية . كلية الزهراوي الجامعية . كربلاء العراق.
[3]علوم التربة والموارد المائية . كلية الزراعة . جامعة القصيم الخضراء . بابل . العراق

---

* Email: almajid1981@gmail.com

الخلاصة

تم دراسة قدرة الازالة اللونية المحفزة ضوئيا للمتراكب النانوي ZnO/MWCNT لازالة صبغة الكريستال البنفسجي من محلولها المائي. المتراكب النانوي حضر بواسطة ترسيب اوكسيد الزنك المتعشق على سطح انابيب الكاربون النانوية متعددة الجدرانMWCNT. باستعمال طريقة الصول–جل حضرت جسميات اوكسيد الزنك النانوي بوجود MWCNT كقالب وشخص بواسطة طيف حيود الاشعة السينية، المجهر الالكتروني الماسح، المجهر الالكتروني النافذوالتي اظهرت شكلا كرويا لاوكسيد الزنك النانويونقطة التعادل الكهربائي لفحص الخواص الفيزيائية. كفاءة الازالة اللونية قيمت بواسطة مفاعل ضوئي غاطسمع مصباح اشعة فوق بنفسجية مغمور في عالق من المتراكب النانوي ZnO/MWCNT ومحلول الصبغة. درست الازالة اللونية لصبغة الكريستال البنفسجي في محلولها المائي في عدة ظروف: تاثير كل من الزمن، وزن العامل المساعد، تركيز الصبغة، درجة الحرارة، الدالة الحامضية الابتدائية لمحلول الصبغة واضافة $S_2O_8^{2-}$ لبيان الظروف المثلى لهذه العملية.اهم النتائج كانت تحضير اوكسيد الزنك النانوي المتعشق على سطح MWCNT وبحجم 10–20 نانومتر مع ازالة لونية عالية ضد صبغة الكريستال البنفسجي. الازالة اللونية الكلية استغرقت 90 دقيقة ووصلت 89.8% عند نصف زمن التفاعل. وزن ZnO/MWCNT بحدود 0.06 غم لكل 100 مل كان الافضل لعملية الازالة اللونية.التفاعل المحفز الضوئي كان اكثر كفاءة عندما يقل تركيز صبغة CV ويطيع حركية لانكماير–هنشلهود، بينما كانت الازالة اللونية لا تقل من 95% ضمن مدى دالة حامضية 6 الى 10.كذلك التفاعل الضوئي المحفز كان متاثرا بوجود ايونات $S_2O_8^{2-}$ حيث كانت الازالة اللونية اكثر كفاءة.

1. Introduction:

The chemical industry and agricultural revolution of the twenty-first century have resulted in the discharge of a wide variety of organic pollutants into water systems. Textile, chemical, and agricultural runoff effluents include synthetic dyestuffs, which are very toxic, bad for the environment, and hazardous to aquatic life. Thus, it has been a top priority for society, the government, and non-governmental organizations for many years. Studies have demonstrated that adding a very small quantity of color to water is quite noticeable and can disrupt aquatic life and food webs since synthetic dyes have the potential to cause cancer [1-3]. For many years, water contaminants have been removed using conventional physico-chemical wastewater treatment techniques as oxidation, ion exchange, and chemical precipitation. The use of expensive synthetic resins and chemicals as well as high energy consumption are some drawbacks of utilizing these technologies, though. Thus, there is a need for novel, inexpensive, and environmentally friendly treatment approaches like photocatalysis [4]. Scientists are interested in "Photocatalysis," the use of semiconductors in decontamination to address environmental problems including pollutant removal from municipal wastewater. In the process of photocatalysis, electrons in the valence bands of semiconductors are stimulated by UV light and moved to their conductive band. Due to the formation of electron-hole pairs, free radicals that can take part in oxidation-reduction processes are generated. The pace of re-union of newly formed electron-hole pairs must be as low as possible and allow for sufficient time for participation in photooxidation-reduction. Additionally, pairs of electron-hole are readily produced in semiconductors with small energy gaps, making photocatalysts preferable [5–11].

Zinc oxide (ZnO) is that semiconductor oxide with significant performance in photocatalysis and has been in the spotlight in latest decade because to its appealing optical and electrical features, as well as its nontoxicity, low cost, and stability. At ambient temperature, it is a semiconductor with an energy gap of 3.37 eV that can only absorb UV light and operate as a photocatalyst. To be cost-effective, in which a photocatalyst work under visible spectrum must be synthesized [18]. As a result, combining zinc oxide doped with conducting materials is a good way to be benefit to use their synergistic effects and improve electron transfere in the composite to enhance the photocatalysis process [12-21].

The probability of charge recombination, which precludes photodegradation, is the fundamental drawback of photocatalysis. This electron-hole recombination can be prevented by mixing MWCNT with other semiconductor nanoparticles or metal oxides. Due to the high charge conductivity of MWCNT, electrons are attracted to it and are less likely to recombine with holes. Since semiconductors are strong electron donors when exposed to light, MWCNT may be thought of as a photo-generated electron acceptor that enhances interfacial electron transport [22–25]. In this research, ZnO nanoparticles were synthesized by sol gel method in the presence of MWCNT as supporter. This composite characterized by some techniques and used for photodecolorization of CV dye in variant conditions. Also, all conditions are contributed with kinetic study to show the optimum parameters that affect this reaction.

2. Experimental part:

2.1 Materials:

Zinc sulfateheptahydrate ($ZnSO_4.7H_2O$) with high purity (99.85%), sodium hydroxide (NaOH) (99%), hydrochloric acid (HCl) (99.8%), Sodium dodecyl sulfate (SDS, 99%), sodium nitrate ($NaNO_3$, 99%),potassium persulfate ($K_2S_2O_8$, 99%) and Crystal violate (CV) with purity 99.9%were purchase from Thompson Baker, India. Multiwall carbon nanotube was supplied from Chemtubes, USA (99.5%). All chemicals were used as supplied from the source without any further purification.

2.2 Preparation of Nanocomposite and MWCNT Modification:

Functionalization of MWCNT is required a noncovalent interaction, where pristine nanotubes were disseminated in a 1 % dilute SDS aqueous solution and ultrasonically modified. The chemical adsorption of SDS molecules on the MWCNT surface causes repulsive force between polar heads exposed in the aqueous solution, inhibiting CNT aggregation. A simple impregnation procedure was used to make the ZnO/MWCNT composites. The process was mixing of SDS modified MWCNT with $ZnSO_4.7H_2O$ solution which is used as a preliminary material of ZnO nanoparticles. A solution of $ZnSO_4.7H_2O$ (7 gm) dissolved in water and MWCNT (0.01 gm) is mixed and dissipated by ultrasonic bath for 30 min to get stable suspension. After that, NaOH diluted solution (0.02 N) is added carefully and dropping on the zinc sulfate-MWCNT solution until the pH is reached 10. The precipitate was filtered and washed with water several time. The white-grey precipitate was dried at 80 C for 24 h and examined by X-Ray Diffractometer (Philips PW 1730/10), SEM and TEM (Zeis Company, Germany).

2.3Determination of point of zero charge (PZC) of ZnO/MWCNT:

The PZC was estimated for ZnO/MWCNT depending on Salt addition method as mentioned in literature [26]. First a solution of 40.0 mL of 0.1 M $NaNO_3$ in a series of 50-mL conical flasks was prepared and then 0.2 g of ZnO/MWCNT was added to. The pH was adjusted as needed with HNO_3 and NaOH solutions to achieve the desired pH in the range of 4, 5, 6, 7, 8, 9, 10, and 11 (±0.1 pH units). pHi was initial values to represent the pH of solution in each flask. Shaking was used (Hetich shaker, Germany) for the solutions at 200 rpm for 24 hours. The final pH values of all solutions in each flask were measured after settling and marked as pHf. PZC was calculated by plotting delta pH=(pHf – pHi) against pHi.

2.4Photocatalytic experiment:

Using CV dye solution under a dipped UV lamp (5 W), the photocatalytic decolorization activity of ZnO/MWCNT nanostructures was evaluated. This procedure was carried out in a UV light chamber with an aqueous CV dye solution at room temperature and pH. First, the combination of photocatalyst and dye solution was agitated in the dark for an hour to allow for adsorption equilibrium with a catalyst dosage of 0.1 gm/100 mL and an initial concentration of 25 ppm. The dye solution and photocatalyst mixture was exposed to UV light with the mercury lamp in order to measure photocatalytic behavior, and samples were taken at regular runs during the irradiation. All tests were conducted in submerged reactions, as shown in Figure 1. Several conditions are studied like effect of reaction time, the ZnO/MWCNT dose, the effect CV dye concentration, initial pH values change, temperature, and effect of the oxidant $K_2S_2O_8$.

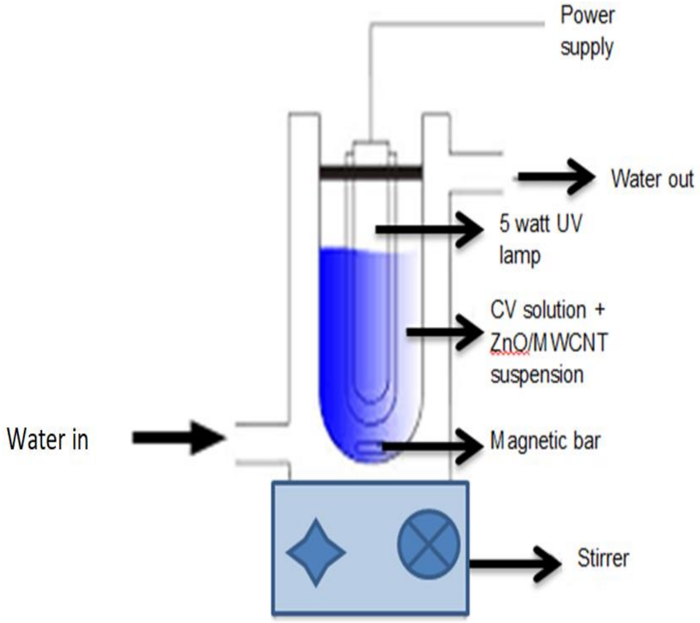

Figure 1: schematic representation of photocatalytic reactor setup.

2. Results and Discussion:

The XRD of ZnO/MWCNT nanocomposite is appeared in Figure 2 and the peaks are indicating the good crystallization of ZnO. The peaks in the XRD spectrum are31.9^o, 34.7^o, 36.5^o, 47.6^o, 56.7^o, 63.1^o, 66.4^o, 68.3^o, and 69.4^{o}crystal planes belong to ZnO with hexagonal structure are given to (100), (002), (101), (102), (110), (103), (200), (112), and (201) crystal planes, respectively and are the identical to the card (JCPDS No. 36-1451). The distinctive peak of MWCNT is difficult to elicit from the spectrum, where it's worth noting that just the ZnO phase appears in the spectrum of ZnO/MWCNT composites. This implies a virtually comparable ZnO structure in the composites as well as a minimal amount of MWCNT. This proves that ZnO's microstructure is unchanged even after MWCNT insertion. When MWCNT is included in the composites, the breadth of the reflections considerably widens, revealing a small crystalline domain size. To estimate the average crystallite size D of nano ZnO in the prepared composite was calculated according to Debye-Scherer formula and it was equal to 14 nm at high intensity peak.

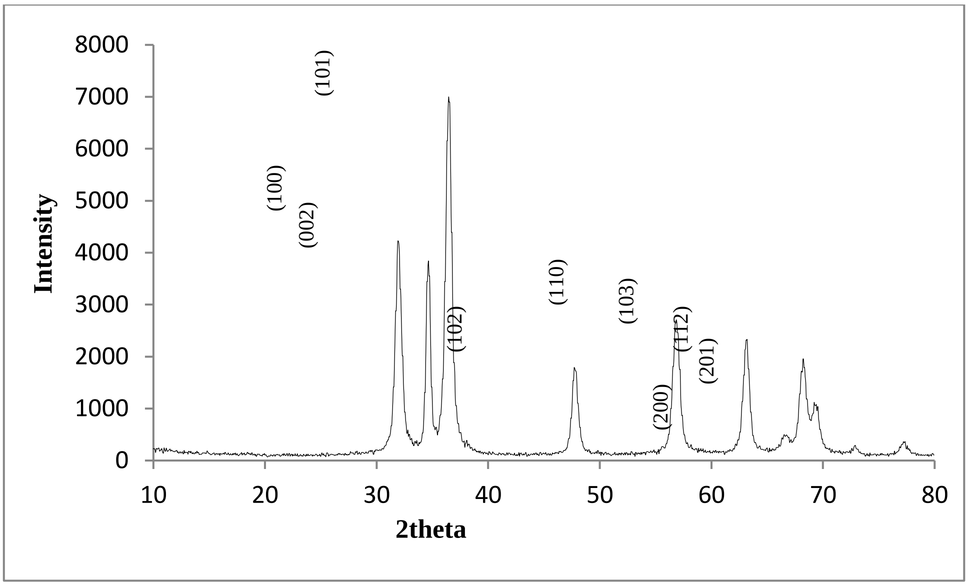

Figure 2: XRD pattern of ZnO/MWCNT nanocomposites.

ZnO/MWCNT nanocomposites can be evaluated for their morphology using FE-SEM. Figure 3a shows a SEM picture of ZnO/MWCNT. CNTs have a diameter of around 20 nm and a length of 600 to 800 nm, as can be observed after processing by imagej program. The ZnO nanoparticles are incorporated with MWCNT and have good dispersion and MWCNTs seem singular and without bundles. Figure 3b shows the TEM picture of ZnO/MWCNT, where the MWCNTs are clearly appeared and ZnO nanoparticles are attached to the structure of MWCNT. The size of ZnO nanoparticles were around 10-20 nm and MWCNT diameter were 15-20 nm. The size of ZnO nanoparticles are approximate to the size that calculated from Scherer's equation.

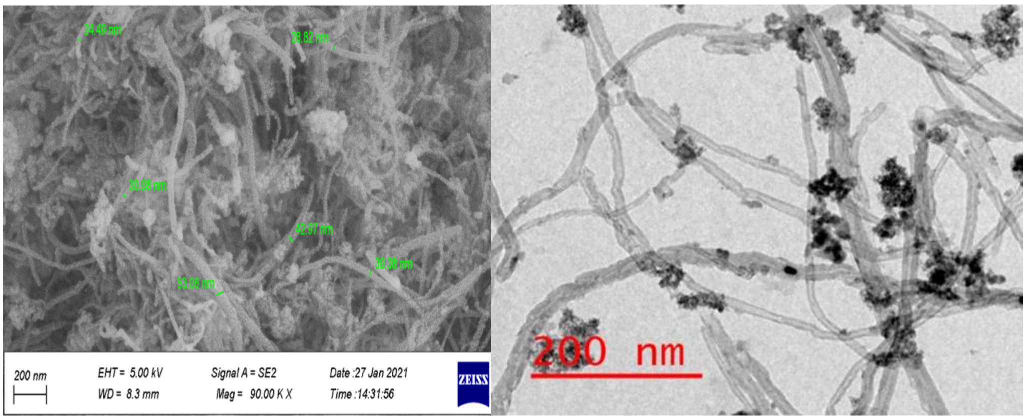

(a) (b)

Figure 3: FESEM (a) and TEM (b) of ZnO/MWCNT nanocomposite.

The photodecolorization of CV dye solution using ZnO/MWCNT and UV light was tested to determine the effect of reaction time, as shown in Figure 4, where 96% of CV dye was constantly degraded after illumination for around 90 minutes. It goes without saying that decolourization increases as the process progresses. The efficiency of decolorization was high reaching 89.8% at half time of reaction then the reaction was appeared slower to vanish the residue of CV concentration. This slow in kinetic of CV dye degradation in the second half time of reaction may be due to the nitrogen atoms converting into oxidized form is difficult. Also, the structure of CV dye has aliphatic short chain and this leading to low ability to scavenge the •OH species, and the byproduct of CV dye is deactivate the active sites of photocatalyst [27].

The photocatalytic effectiveness of ZnO is determined by oxygen vacancies and imperfections. These vacancies and defects reduce the number of induced electrons and holes recombination, which is beneficial. Under UV irradiation, O_2 promotes the oxidation of organic molecules by producing additional radicals. Also MWCNTs own the ability to act as photosensitizers for the semiconductor ZnO. Furthermore, MWCNTs can operate as a dispersion agent, preventing ZnO nanoparticles from clumping together, resulting in a greater active surface area of the nanocomposite catalyst. Thus the final results are the CV photocatalytic degradation is much improved [28, 29].

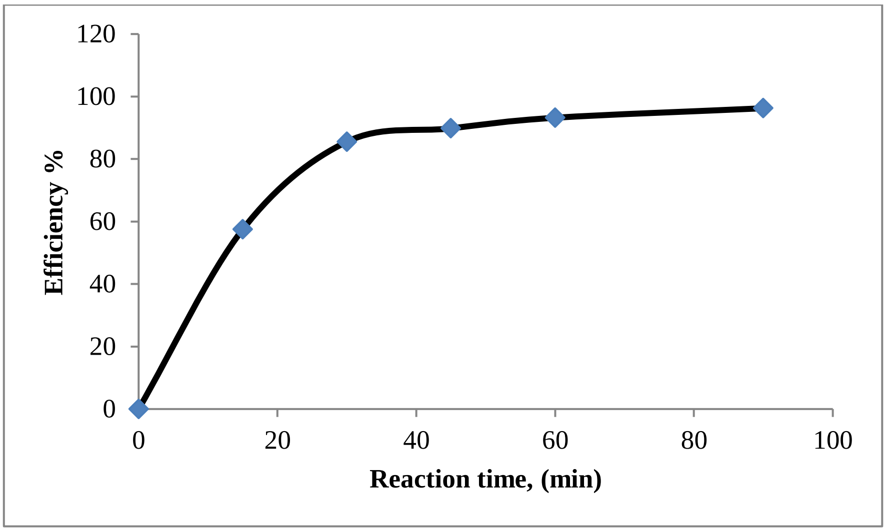

Figure 4: the photodecolorization of CV relation with time in the presence of ZnO/MWCNT and the reaction conditions are 15 ppm of crystal violate, pH=6.1, catalyst dose= 0.04 gm in 100 ml. T=303 K.

The amount of catalyst used as a slurry in the CV solution to study the deterioration significantly impacted and modified the photocatalysis. In this condition, we studied the effect of different doses of catalyst ranging from 0.01 g to 0.09 g per 100 mL to evaluate CV removal efficiency from its solution using ZnO/MWCNT. All conditions were remained constant like the concentration of CV dye solution (15 mg/L) and ambient pH and temperature. The degradation efficiency of ZnO/MWCNT of CV dye is demonstrated in Figure 5, which is showing the photocatalysis efficiency of degradation improved with increasing catalyst amounts. When the catalyst dose was increased, the photocatalytic reaction was faster in degradation. This could be due to an increase in the number of active sites relative to the amount of photocatalyst increasing. And that is found out the rate of breakdown is dependent on the amount of catalyst presence. The reaction mixture with high catalyst dose of 0.09 g cannot be adequately homogenized at a given agitation rate, the efficiency was low. Also, the larger catalyst dose prevents irradiation from entering into the solution, where finally, the active sites are turned to be inactive, leading to low catalytic efficiency and the catalytic activity is reduced. According to the kinetics of ZnO/MWCNT behavior in case of changing the weight of the photocatalyst, the final results is obtained for k_{app} with close results as reported [30], as shown in the stacked figure in Figure 5, which is show the relation of k_{app} with photocatalyst weight.

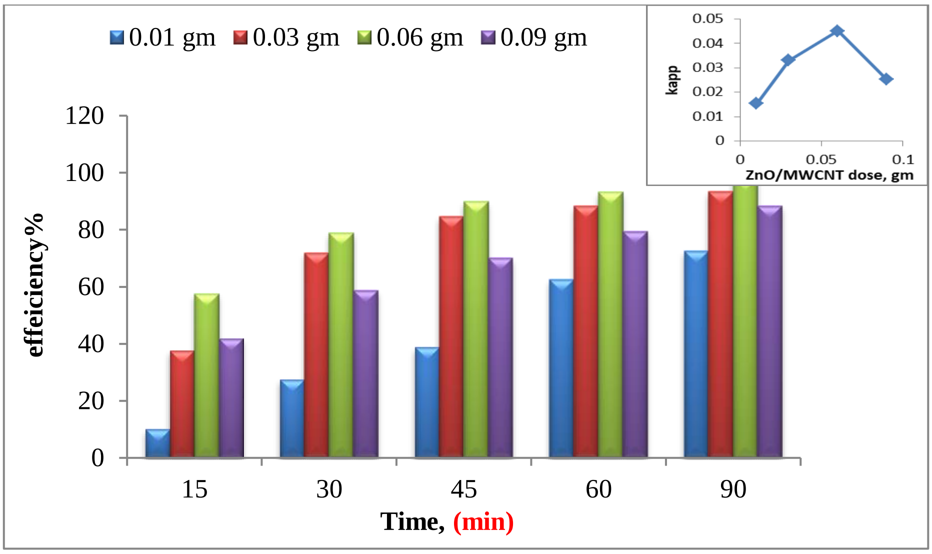

Figure 5: effect of ZnO/MWCNT dose photodecolorization of CV dye, where the concentration was 15 ppm of crystal violate, pH=6.1 and T=303 K and the stacked figure is the relation of kapp with ZnO/MWCNT dose.

A pseudo-first order kinetics was used to assess the rate of CV degradation by ZnO-MWCNT. The rate constant may be calculated using the following equation [31].

$$\ln\frac{C_o}{C} = k.t \qquad ....(1)$$

Where k: is the photocatalytic reaction's rate constant, C_o is the CV dye's initial concentration, and C_t is the CV dye's concentration at time t. The photocatalytic breakdown of CV by ZnO/MWCNT validates the fractional order reaction. The kinetic of photocatalysis of CV dye related as dependent on irradiation time follows an exponential decay like shape. In addition, in case of plot the $\ln(C_o/C)$ against reaction time for the entire dyes in the optimal conditions was likewise a linear and for all concentrations, implying that the photodegradation mechanism followed pseudo-first-order reaction kinetics as reported [32, 33].The kinetic of photodecolorization of CV dye in aqueous solution was studied in different concentrations 5, 10, 15, and 25 ppm. This is studying of the effect of concentration alteration on the rate of photocatalytic reaction. We found that, there is an inverse relation between rate and its concentration. As an explanation, when CV concentration was low, the number of active sites are unfilled, thus the activity of photodecolorization was high. But at high concentration of dye the rate of photodecolorization was low, because of full covering of the surface and the dye made a screen effect and depleted of UV light and preventing of electron-hole pair separation, and thus the efficiency is low when CV concentration is high according to inner filter effect as reported [34-36].

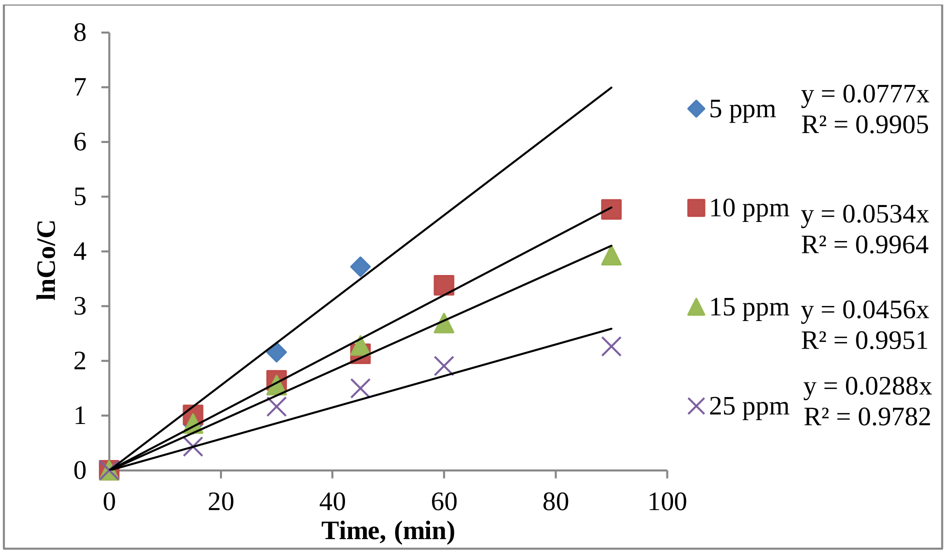

Figure 6: effect of CV concentration on the photodecolorization by ZnO/MWCNT, where pH=6.1, ZnO/MWCNT = 0.06 gm in 100 ml and T=303 K.

For the photocatalytic process, which is demonstrated by the substrate's adsorption characteristics on the photocatalyst surface, the Langmuir-Hinshelwood rate equation is hugely beneficial. This formula has been widely used for prediction the photocatalytic degradation of various organic compounds in photocatalysts like ZnO/MWCNT suspensions under UV light illumination. The Langmuir-Hinshelwood equation can be expressed using following equation[34-37]:

$$\text{rate} = -\frac{dC}{dt} = \frac{k_{L\_H}.K.C}{1+K_{ads}.C} \qquad \text{..........(2)}$$

, and we can obtain the equation:

$$\frac{1}{k_{app}} = \frac{1}{k_{L\_H}.K} + \frac{C_o}{k} \qquad \text{..........(3)}$$

The coefficients ($k_{L–H}$ and K_{ads}) are describing the reaction rate on the surface that is determining the degradation events. Also, its benefit for explaining the case of pre-equilibrium adsorption that is happen for organic molecules. These molecules are adsorbed at the surface of photocatalyst in a monolayer and are very affected by aqueous solution interface. In terms of $k_{L–H}$ takes into account the influence of light intensity, while K_{ads} expresses the equilibrium constant for rapid adsorption-desorption processes between a surface monolayer and a bulk solution [30, 37]. By plotting the inverse of k_{app} against initial concentration to give straight line in the concentration 5, 10, 15 and 25 ppm, where the relation is showed in Figure 7 and this kinetic is obeyed Langmuir–Hinshelwood model. The parameters that obtained from this model were k=0.933 mg/L. min and K=0.1445 L/mg.

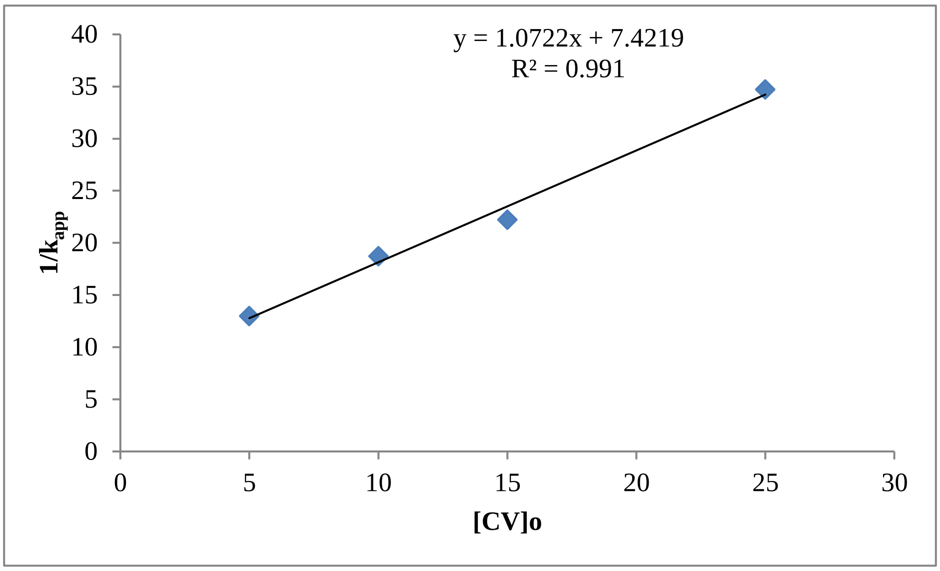

Figure 7: Langmuir–Hinshelwood plot of photodecolorization of various CV initial concentrations.

The primary factor affecting how quickly dye degrades on the surface of the photocatalyst is the pH. Effects of changing the pH of the dye solution were investigated. Additionally, by adding small amounts of 0.1 M HCl and 0.1 M NaOH, several pH values in the range of 5 to 10 were tested in order to assess the dye degradation efficiency. The findings are shown in Figure 8. CV degradation efficiency was found to be good in an acidic media, whereas it was found to be high in a basic media. With ZnO/MWCNT, CV degradation efficiency increased from 95 percent at pH 5 to 98 percent at pH 6, and reached 97 percent pH 10. As marked values of decolorization efficiency in Figure 8.

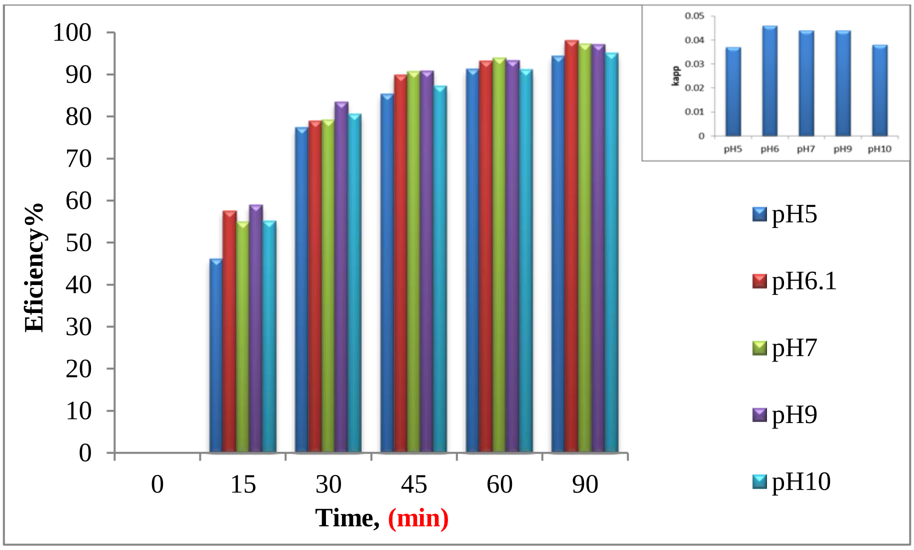

Figure 8: Effect of pH on photodecolorization of CV dye solution and the experimental conditions are 15 ppm of CV, ZnO/MWCNT dose = 0.06 gm in 120 ml and T=303 K.

Due to MWCNT modification, ZnO/MWCNT nanocomposite has the capacity to function with high efficiency over a range of pH. The surface charge photocatalyst is negative at basic pH due to the significant interaction between OH and metal at alkaline pH. Acidity also affects dye cations because they include an ionized group (the amine group), which causes electrostatic repulsion. This making pushed further dyes molecules towards the catalyst surface. Hence the amount of reducing electrons increased, resulting in excellent CV dye degradation. At alkaline pH, the most common species are hydroxyl radicals; the dye concentration has photocatalyticaly decreased that results from the amount of OH radicals are dominant and have high-oxidation-potential [38]. Another aspect was the pzc of ZnO/MWCNT nanocomposite estimated according to the relation of pH_f-pHi against pHi and the pzc equal to 7.6 as plotted in Figure 9. Within the reaction time during 90 minutes of contact, the decolorization percent of CV increased for neutral and basic medium. When the initial pH of CV solution is less than the point of zero charge as in pH=5, the surface charge of the MWCNTs is positive, and that diminished the capacity of interaction with cation of CV dye. While pH rises, the negative charge on the ZnO/MWCNT surface interacts electrostatically with CV. On other hand, the pzc is 9 for pure ZnO, but the combination with MWCNTs reduce the pzc and in the maintenance of photodecolorization ability to be not less than 95% in pH range 6-10 [39,40].

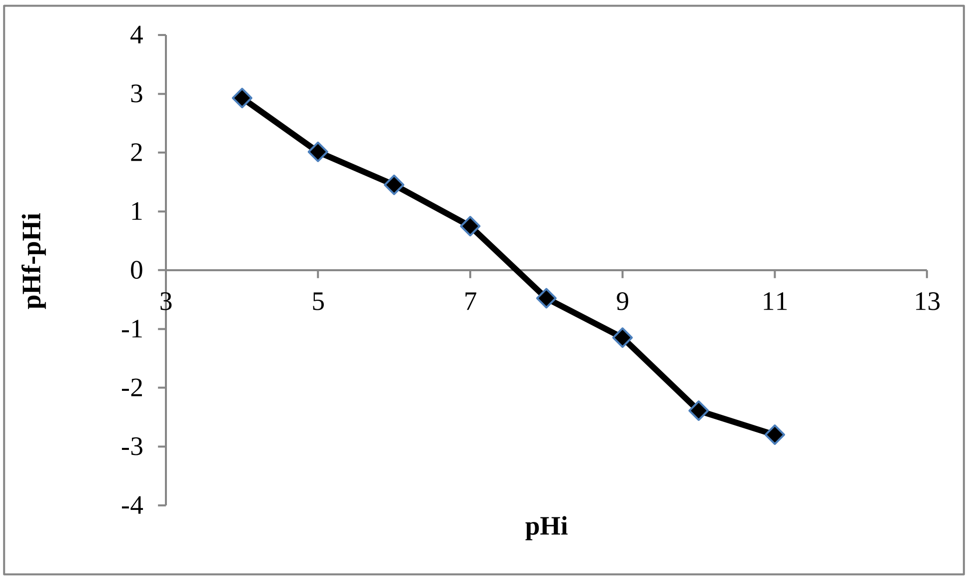

Figure 9: the PZC plot of ZnO/MWCNT nanocomposite

It is possible to determine whether or not a photocatalytic reaction is influenced by varying the reaction's temperature. Our investigation used temperatures of 293, 303, and 313 K. In order to measure the absorption, a spectrophotometer was used at various temperatures while the dye solution was exposed to UV light for 90 minutes at 15-minute intervals. The results are depicted in Figure 10 and demonstrate how photodegradation was clearly more successful at higher temperatures. As can be shown, when ZnO/MWCNT are present and the temperature is raised, the percentage of degradation for CV dye also increases. The degradation reaction can be expected to be an endothermic process because of the effect of temperature on the quantity of decolorization of CV solution was positive. With rising temperature, ZnO/MWCNT photocatalyst enhanced dye degradation, which could be due to three main motives: In beginning, with rising the temperature causes molecules to move quicker, creating a higher interaction between CV and ZnO/MWCNT nanocomposite. As a result, the likelihood of dye molecules degrading on the photocatalyst increases. Second, higher temperatures cause an increase in free radical generation and the creation of bubbles in dye solutions. Third, the high relative temperature reduces the possibility the pair of electron-hole recombination, resulting in improved dyes removal of the photocatalyst [41, 42].

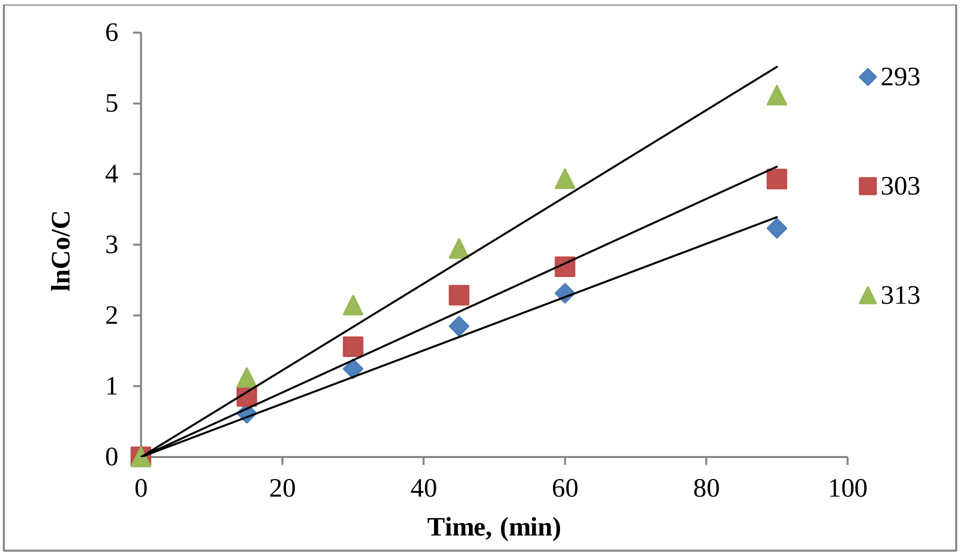

Figure 10: effect of temperature on photodecolorization of CV dye solution, where the conditions are 15 ppm of CV, pH=6.1 and ZnO/MWCNT dose= 0.06 gm in 120 ml.

According to Figure 11, the rate constant (k_{app}) of photodecolorization of CV dye was compatible with Arrhenius temperature-dependence and it increased with temperature exponentially as in equation 4 [43].

$$k=A\ e^{-Ea/RT} \quad \text{..........(4)}$$

Where k is the apparent rate constant (temperature-independence), Ea is the apparent activation energy, T is temperature in Kelvin in which the reaction was conducting, R is the gas constant (8.314 J/K. mol).

The result showed the increase of rate constant of reaction as temperature rising. The activation energy was calculated from the slope of lnk against 1000/T and straight line was obtained and the slope=-Ea/R=-2.2229 and the activation energy was 18.5 kJ/mol. This value of apparent activation energy is entirely the total activation energy that contributed by adsorption and photocatalytic degradation of CV.

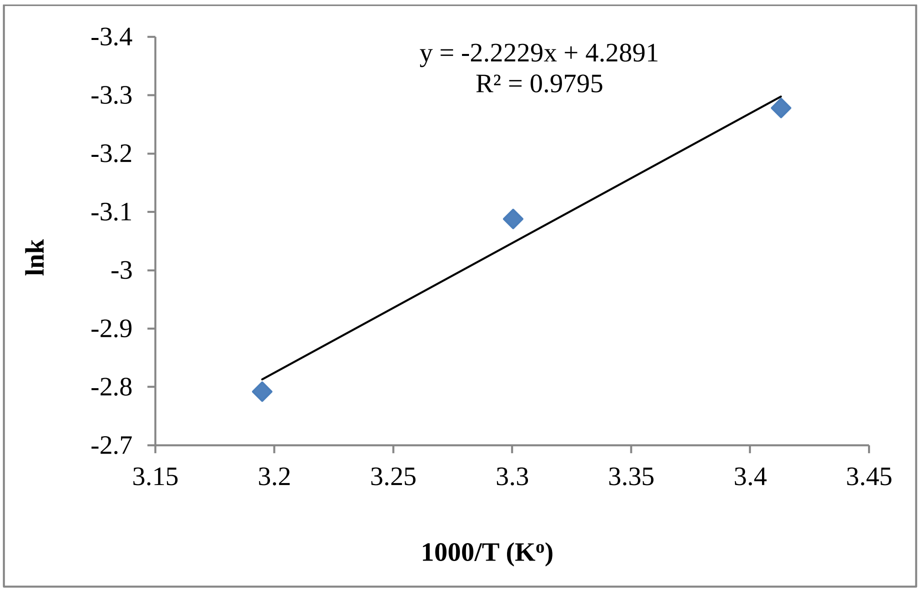

Figure 11: Arrhenius plot of lnk with the reciprocal of temperature for photodecolorization of CV dye by ZnO/MWCNT.

In Figure 12 the effect of $S_2O_8^{2-}$ on the photodecolorization of CV dye in aqueous solution in the presence of ZnO/MWCNT was studied. $S_2O_8^{2-}$ addition under study was 0, 0.5, and 1 ml of 0.01 M $K_2S_2O_8$ and the decolorization efficiency was increased in this range in comparison to the reaction without $S_2O_8^{2-}$. The removal efficiency of CV dye was remarkably improved by adding $S_2O_8^{2-}$, where the reaction time reduced to reach efficiency 99% in 60 min. $S_2O_8^{2-}$ is strong electron acceptors, and it has the ability of capturing photogenerated electron in conduction band(e_{CB}^{-}), working as scavenger as in equation 5:

$$S_2O_8^{2-} + e_{CB}^{-} \rightarrow SO_4^{\bullet -} + SO_4^{2-} \qquad \text{.........(5)}$$

This reaction elevate holes in valance band h_{VB}^{+} concentration and subsequently increased the concentration of $^{\bullet}OH$ on the surface of photocatalyst [44]. Exposing $S_2O_8^{2-}$ to UV light lead to photolysis will generate additional $SO_4^{\bullet -}$, according to reactions photolysis equation 6:

$$S_2O_8^{2-} + hv \rightarrow 2SO_4^{\bullet -} \qquad \text{.........(6)}$$

The above equation products, increases of the charge separation on photocatalyst surface and so on the increasing of •OH production by the generated $SO_4^{\bullet -}$could explain the high efficiency of photodecolorization of CV dye by prepared photocatalyst ZnO/MWCNT. Thus the addition of $S_2O_8^{2-}$ enhances the photodecolorization to reach 100% removal in addition of low concentration of $S_2O_8^{2-}$. The k_{app} is increased as follow (0.0456, 0.0617 and 0.0841 min^{-1}) in addition of 0, $5*10^{-5}$ and 10^{-4} M of $S_2O_8^{2-}$ respectively as in Figure 12. Higher effects had obtained by the $S_2O_8^{2-}$concentration increasing may be due to $S_2O_8^{2-}$ photolysis increase the $SO_4^{\bullet -}$generation [45].

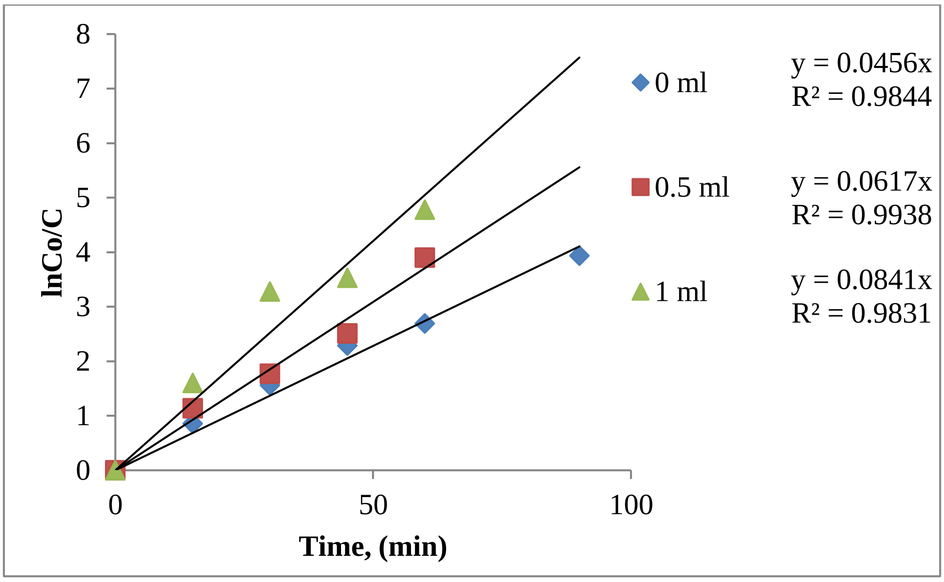

Figure 12: the effect of $S_2O_8^{2-}$addition on the kinetic of CV photodecolorization by ZnO/MWCNT.

4. Conclusions:

The MWCNT/ZnO nanocomposite was synthesized using the sol-gel process, which produced an extremely thin powder with a nanometric scale of 10–20 nm. In this procedure, ZnO nanoparticles were distributed over MWCNT in an aqueous solution and were synthesized using MWCNTs as a suitable template. The composite was quite effective in photodecolorizing CV dye, and it took 90 minutes to complete the process. The catalyst dose directly impacted the photodecolorization efficiency up to a high dose and made an inner filter; the ideal value was 0.06 gm/100 mL. Above pH=5 and in the broad pH=6–10 range, efficiency improved. The photodecolorization accelerated with rising temperature. S_2O8_2 increased photodecolorization and shortened the response time to 60 minutes.

Conflict of interest: The authors are declaring there is no conflict of interest regarding this manuscript.

References

[1] A. W. Yibeltal, B. B. Beyene, S. Admassie, and A. M. Taddesse, “MWCNTs/AG-ZnO nanocomposite for efficient photocatalytic degradation of Congo red,” *Bulletin of the Chemical Society of Ethiopia*, vol. 34, no. 1, pp. 55–66, 2020.

[2] S. Chatterjee, D. S. Lee, M. W. Lee, and S. H. Woo, “Enhanced adsorption of congo red from aqueous solutions by chitosan hydrogel beads impregnated with cetyltrimethyl ammonium bromide.” *Bioresource Technology*, vol. 100, no. 11, pp. 2803-2809, 2009, doi: 10.1016/j.biortech.2008.12.035.

[3] Atiya, M. A., M-Ridha, M. J, & Saheb, M. A. “Removal of Aniline Blue from Textile Wastewater using Electrocoagulation with the Application of the Response Surface Approach”. *Iraqi Journal of Science*, 61(11), 2797–2811, 2020.

[4] G. Annadurai, R. Juang, P. Yen, and D. Lee, “Use of thermally treated waste biological sludge as dye absorbent.” *Advances in Environmental Research*, vol. 7, no. 3, pp. 739-744, 2003, doi: 10.1016/s1093-0191(02)00044-8.

[5] Muhi-Alden, Y. Y., and Saleh, K. A. “Removing of Methylene Blue Dye from its Aqueous Solutions Using Polyacrylonitrile/Iron Oxide/Graphene Oxide”. *Iraqi Journal of Science*, 63(6), 2320-2330, 2022.

[6] S. Okeil, J. Krausmann, I. Dönges, S. Pfleger, J. Engstler, and J. J. Schneider, “ZnS/ZnO@CNT and ZnS@CNT nanocomposites by gas phase conversion of ZnO@CNT. A systematic study of their photocatalytic properties.” *Dalton Transactions*, vol. 46, no. 16, pp. 5189-5201, 2017, doi: 10.1039/c7dt00407a.

[7] D. Kanakaraju, B. D. Glass, and M. Oelgemöller, “Titanium dioxide photocatalysis for pharmaceutical wastewater treatment.” *Environmental Chemistry Letters*, vol. 12, no. 1, pp. 27-47, 2013, doi: 10.1007/s10311-013-0428-0.

[8] H. Zangeneh, A. Zinatizadeh, M. Habibi, M. Akia, and M. Hasnain Isa, “Photocatalytic oxidation of organic dyes and pollutants in wastewater using different modified titanium dioxides: A comparative review.” *Journal of Industrial and Engineering Chemistry*, vol. 26, pp. 1-36, 2015, doi: 10.1016/j.jiec.2014.10.043.

[9] S. Li, M. Zhang, Y. Gao, B. Bao, and S. Wang, “ZnO–Zn/CNT hybrid film as light-free nanocatalyst for degradation reaction.” *Nano Energy*, vol. 2, no. 6, pp. 1329-1336, 2013, doi: 10.1016/j.nanoen.2013.06.015.

[10] C. Han, M.-Q. Yang, B. Weng, and Y.-J. Xu, “Improving the photocatalytic activity and anti-photocorrosion of semiconductor ZnO by coupling with versatile carbon.” *Physical Chemistry Chemical Physics*, vol. 16, no. 32, p. 16891, 2014, doi: 10.1039/c4cp02189d.

[11] A. Mills, S. Le Hunte, “An overview of semiconductor photocatalysis*”. Journal of photochemistry and photobiology A: Chemistry*, vol. 108, no. 1, pp.1-35, 1997, doi.org/10. 1016/S1010-6030(97)00118-4.

[12] M. H. A. Azqhandi, B. Vasheghani F., F. Rajabi, and M. Keramati, “Synthesis of Cd doped ZnO/CNT nanocomposite by using microwave method: Photocatalytic behavior, adsorption and kinetic study.” *Results in Physics*, vol. 7, pp. 1106-1114, 2017, doi: 10.1016/j.rinp.2017.02.033.

[13] P. Liu, Y. Guo, Q. Xu, F. Wang, Y. Li, and K. Shao, “Enhanced photocatalytic performance of ZnO/multi-walled carbon nanotube nanocomposites for dye degradation.” *Ceramics International*, vol. 40, no. 4, pp. 5629-5633, 2014, doi: 10.1016/j.ceramint.2013.10.157.

[14] J. Qu, Q. Cong, and C. Luo, “Synthesis of carbon nanotube/ZnO nanocomposites using absorbent cotton and their photocatalytic activity.” *Micro & Nano Letters*, vol. 7, no. 10, pp. 1064-1068, 2012, doi: 10.1049/mnl.2012.0619.

[15] S. Ma, J. Xue, Y. Zhou, and Z. Zhang, “Photochemical synthesis of ZnO/Ag2O heterostructures with enhanced ultraviolet and visible photocatalytic activity." *J. Mater. Chem. A*, vol. 2, no. 20, pp. 7272-7280, 2014, doi: 10.1039/c4ta00464g.

[16] H. Bai, X. Zan, L. Zhang, and D. D. Sun, "Multi-functional CNT/ZnO/TiO_2 nanocomposite membrane for concurrent filtration and photocatalytic degradation." *Separation and Purification Technology*, vol. 156, pp. 922-930, 2015, doi: 10.1016/j.seppur.2015.10.016.

[17] H.- Y. He, "Photoinduced superhydrophilicity and high photocatalytic activity of ZnO–reduced graphene oxide nanocomposite films for self-cleaning applications." *Materials Science in Semiconductor Processing*, vol. 31, pp. 200-208, 2015, doi: 10.1016/j.mssp.2014.11.029.

[18] H. He, J. Fei, and J. Lu, "High photocatalytic and photo-Fenton-like activities of ZnO–reduced graphene oxide nanocomposites in the degradation of malachite green in water." *Micro & Nano Letters*, vol. 10, no. 8, pp. 389-394, 2015, doi: 10.1049/mnl.2014.0551.

[19] J. Rodrigues, "One-step synthesis of ZnO decorated CNT buckypaper composites and their optical and electrical properties." *Materials Science and Engineering: B,* vol. 195, pp. 38-44, 2015, doi: 10.1016/j.mseb.2015.01.009.

[20] R. Saravanan, V. Gupta, E. Mosquera, and F. Gracia, "Preparation and characterization of V_2O_5/ZnO nanocomposite system for photocatalytic application." *Journal of Molecular Liquids*, vol. 198, pp. 409-412, 2014, doi: 10.1016/j.molliq.2014.07.030.

[21] Q. T. H. Ta, G. Namgung, and J.-S. Noh, "Facile synthesis of porous metal-doped ZnO/g-C_3N_4 composites for highly efficient photocatalysts." *Journal of Photochemistry and Photobiology A: Chemistry*, vol. 368, pp. 110-119, 2019, doi: 10.1016/j.jphotochem.2018.09.049.

[22] T. A. Saleh and V. K. Gupta, "Functionalization of tungsten oxide into MWCNT and its application for sunlight-induced degradation of rhodamine B." *Journal of Colloid and Interface Science*, vol. 362, no. 2, pp. 337-344, 2011, doi: 10.1016/j.jcis.2011.06.081.

[23] E. Bartfai, K. Nemeth, B. E. Mrabate, M. Udayakumar, K. Hernadi, and Z. Nemeth, "Synthesis, Characterization and Photocatalytic Efficiency of ZnO/MWCNT Nanocomposites Prepared Under Different Solvent Conditions." *Journal of Nanoscience and Nanotechnology*, vol. 19, no. 1, pp. 422-428, 2019, doi: 10.1166/jnn.2019.15773.

[24] V. Subramanian, E. E. Wolf, and P. V. Kamat, "Catalysis with TiO2/Gold Nanocomposites. Effect of Metal Particle Size on the Fermi Level Equilibration." *Journal of the American Chemical Society*, vol. 126, no. 15, pp. 4943-4950, 2004, doi: 10.1021/ja0315199.

[25] X. Wang, "Synthesis of novel nanomaterials and their application in efficient removal of radionuclides." *Science China Chemistry*, vol. 62, no. 8, pp. 933-967, 2019, doi: 10.1007/s11426-019-9492-4.

[26] E. N. Bakatula, D. Richard, C. M. Neculita, and G. J. Zagury, "Determination of point of zero charge of natural organic materials." *Environmental Science and Pollution Research*, vol. 25, no. 8, pp. 7823-7833, 2018, doi: 10.1007/s11356-017-1115-7.

[27] C. G. Maia, A. S. Oliveira, E. M. Saggioro, and J. C. Moreira, "Optimization of the photocatalytic degradation of commercial azo dyes in aqueous TiO2 suspensions." *Reaction Kinetics, Mechanisms and Catalysis*, vol. 113, no. 1, pp. 305-320, 2014, doi: 10.1007/s11144-014-0737-8.

[28] M. Moradi, M. Haghighi, and S. Allahyari, "Precipitation dispersion of Ag–ZnOnanocatalyst over functionalized multiwall carbon nanotube used in degradation of Acid Orange from wastewater." *Process Safety and Environmental Protection*, vol. 107, pp. 414-427, 2017, doi: 10.1016/j.psep.2017.03.010.

[29] B. Arora and P. Attri, "Carbon Nanotubes (CNTs): A Potential Nanomaterial for Water Purification." *Journal of Composites Science,* vol. 4, no. 3, p. 135, 2020, doi: 10.3390/jcs4030135.

[30] K. A. Isai and V. S. Shrivastava, "Photocatalytic degradation of methylene blue using ZnO and 2%Fe–ZnO semiconductor nanomaterials synthesized by sol–gel method: a comparative study." *SN Applied Sciences*, vol. 1, no. 10, 2019, doi: 10.1007/s42452-019-1279-5.

[31] M. Singh, A. Kumar, and V. Krishnan, "Influence of different bismuth oxyhalides on the photocatalytic activity of graphitic carbon nitride: a comparative study under natural sunlight." *Materials Advances*, vol. 1, no. 5, pp. 1262-1272, 2020, doi: 10.1039/d0ma00294a.

[32] S. Alkaykh, A. Mbarek, and E. E. Ali-Shattle, "Photocatalytic degradation of methylene blue dye in aqueous solution by $MnTiO_3$ nanoparticles under sunlight irradiation." *Heliyon*, vol. 6, no. 4, 2020, doi: 10.1016/j.heliyon.2020.e03663.

[33] F. Sanakousar, C. Vidyasagar, V. Jiménez-Pérez, and K. Prakash, "Recent progress on visible-light-driven metal and non-metal doped ZnO nanostructures for photocatalytic degradation of organic pollutants." *Materials Science in Semiconductor Processing*, vol. 140, p. 106390, 2022, doi: 10.1016/j.mssp.2021.106390.

[34] V. Yadav, P. Verma, H. Sharma, S. Tripathy, and V. K. Saini, "Photodegradation of 4-nitrophenol over B-doped TiO_2 nanostructure: effect of dopant concentration, kinetics, and mechanism." *Environmental Science and Pollution Research*, vol. 27, no. 10, pp. 10966-10980, 2020, doi: 10.1007/s11356-019-06674-x.

[35] Bhawna, B. P. Majee, V. Choudhary, R. Prakash, and A. K. Mishra, "Hydrothermally grown ZnO nanoparticles for photodegradation of textile dye." *AIP Conference Proceedings*, 2019, doi: 10.1063/1.5098627.

[36] A. Zuorro, R. Lavecchia, M. M. Monaco, G. Iervolino, and V. Vaiano, "Photocatalytic Degradation of Azo Dye Reactive Violet 5 on Fe-Doped Titania Catalysts under Visible Light Irradiation." 2019, doi: 10.20944/preprints201906.0233.v1.

[37] A. K. Tallapaka, J. Thati, and S. Chintha, "Oxidative Photocatalytic Degradation of Methylene Blue in Wastewater." *Recent Trends in Waste Water Treatment and Water Resource Management*, pp. 119-127, 2020, doi: 10.1007/978-981-15-0706-9_12.

[38] K. KenchappaSomashekharappa and S. V. Lokesh, "Hydrothermal Synthesis of K2Ti6O13 Nanotubes/Nanoparticles: A Photodegradation Study on Methylene Blue and Rhodamine B Dyes." *ACS Omega*, vol. 6, no. 11, pp. 7248-7256, 2021, doi: 10.1021/acsomega.0c02087.

[39] F. S. Aljohani, "Water Treatment from MB Using Zn-Ag MWCNT Synthesized by Double Arc Discharge." *Materials*, vol. 14, no. 23, p. 7205, 2021, doi: 10.3390/ma14237205.

[40] F. Hosseini, A. Kasaeian, F. Pourfayaz, M. Sheikhpour, and D. Wen, "Novel ZnO-Ag/MWCNT nanocomposite for the photocatalytic degradation of phenol." *Materials Science in Semiconductor Processing*, vol. 83, pp. 175-185, 2018, doi: 10.1016/j.mssp.2018.04.042.

[41] Y. Meng, S. Xia, G. Pan, J. Xue, J. Jiang, and Z. Ni, "Preparation and photocatalytic activity of composite metal oxides derived from Salen-Cu(II) intercalated layered double hydroxides." *Korean Journal of Chemical Engineering*, vol. 34, no. 8, pp. 2331-2341, 2017, doi: 10.1007/s11814-017-0135-9.

[42] A. Yamamoto, Y. Mizuno, K. Teramura, T. Shishido, and T. Tanaka, "Effects of reaction temperature on the photocatalytic activity of photo-SCR of NO with NH3 over a TiO_2 photocatalyst." *Catalysis Science & Technology*, vol. 3, no. 7, p. 1771, 2013, doi: 10.1039/c3cy00022b.

[43] X. Y. Li, Q. Z. Luo, J. An, and D. S. Wang, "The Kinetics and Activation Energy of Photocatalytic Degradation of Phenol by TiO_2 and TiO_2/ PANI Photocatalyst under UV Irradiation." *Advanced Materials Research*, vol. 430, pp. 57-60, 2012, doi: 10.4028/www.scientific.net/amr.430-432.57.

[44] G. K. Dinesh and S. Chakma, "Mechanistic investigation in degradation mechanism of 5-Fluorouracil using graphitic carbon nitride." *UltrasonicsSonochemistry*, vol. 50, pp. 311-321, 2019, doi: 10.1016/j.ultsonch.2018.09.032.

[45] S. Khan, X. He, J. A. Khan, H. M. Khan, D. L. Boccelli, and D. D. Dionysiou, "Kinetics and mechanism of sulfate radical- and hydroxyl radical-induced degradation of highly chlorinated pesticide lindane in UV/peroxymonosulfate system." *Chemical Engineering Journal*, vol. 318, pp. 135-142, 2017, doi: 10.1016/j.cej.2016.05.150.